Quantitation of ^{99m}Tc-DPD uptake in patients with transthyretin-related cardiac amyloidosis

James C. Ross[1,2], David F. Hutt[1], Maria Burniston[1,3], Joanne Page[1,4], Jennifer A. Steeden[5], Julian D. Gillmore[1], Ashutosh D. Wechalekar[1], Philip N. Hawkins[1], Marianna Fontana[1]

[1]National Amyloidosis Centre, UCL Medical School (Royal Free Campus), London, UK

[2]Institute of Nuclear Medicine, University College London Hospitals NHS Foundation Trust, London, UK

[3]Nuclear Medicine Department, Nuclear Medicine, Barts Health NHS Trust, London, UK

[4]Nuclear Medicine Department, Royal Free London NHS Foundation Trust, London, UK

[5]UCL Centre for Cardiovascular Imaging, University College London, London, UK

Abstract

Purpose

Transthyretin (ATTR) amyloidosis is a rare but serious infiltrative disease associated with a wide spectrum of morphologic and functional cardiac involvement. ^{99m}Tc-labelled 3,3-diphosphono-1,2-propanodicarboxylic acid (DPD), initially developed as a bone-seeking radiotracer, is remarkably sensitive for imaging cardiac ATTR amyloid deposits. Our aim was to investigate the feasibility and utility of estimating ^{99m}Tc-DPD uptake in myocardial tissue; this has the potential to yield reliable quantitative information on cardiac amyloid burden, which is urgently required to monitor disease progression and response to novel treatments.

Methods

Three methods of quantitation were developed and tested on 74 patients with proven cardiac ATTR amyloidosis who had recently undergone ^{99m}Tc-DPD planar whole-body imaging and SPECT-CT. Quantitative results were compared to measurements of extracellular volume fraction (ECV) by cardiac magnetic resonance imaging, a validated technique for measuring amyloid burden.

Results

An experienced clinician graded uptake using a widely-used visual scoring system as 1 (n = 15), 2 (n = 39), or 3 (n = 20). Linear correlations between the SPECT and ECV data ($p < 0.001$) were demonstrated. None of the methods showed that ^{99m}Tc-DPD uptake in the heart was significantly greater in patients with grade-3 uptake than in those with grade-2 uptake.

Conclusions

Quantitation of ^{99m}Tc-DPD uptake in cardiac transthyretin amyloid deposits is complex and is hindered by competition for radiotracer with amyloid in skeletal muscle. The latter underlies differences in uptake between grade-2 and grade-3 patients, not cardiac uptake.

Key words: amyloidosis, ATTR, cardiology, DPD, quantitation, SPECT

Corresponding author:

James C. Ross

Institute of Nuclear Medicine T05, 235 Euston Road, London, NW1 2BU, United Kingdom

Telephone: +44 (0)203 4470522

Email: james.ross8@nhs.net

Introduction

Amyloidosis

The term amyloidosis refers to a heterogeneous group of rare diseases which are characterised by extracellular deposition and accumulation of normally-soluble plasma proteins in insoluble, fibrillar forms [1]. Amyloid deposits can build up in individual tissues and organs or deposition can be systemic (i.e. widespread). Symptoms occur when there is a sufficient amount of amyloid present to disrupt the normal structures and functions of affected sites.

More than 30 proteins are known to form amyloid fibrils in humans [2]. The most common types are acquired immunoglobulin light-chain (AL) and transthyretin (ATTR). ATTR amyloidosis is either acquired, known as wild-type ATTR amyloidosis ($ATTR_{wt}$), or hereditary, known as mutant-type ATTR amyloidosis ($ATTR_{mt}$), denoting the many possible mutations in the transthyretin gene [3]. Although the diagnosis of amyloidosis is rare—500 to 1000 new cases are diagnosed in the U.K. each year—the true prevalence is unknown.

Cardiac involvement is a significant factor in determining prognoses and treatments for patients with systemic amyloidosis. Cardiac amyloidosis presents as a restrictive cardiomyopathy due to the presence of amyloid deposits in the myocardium, which is characterised by restricted ventricular filling. Survival is typically poorer for AL patients (6–12 months) than it is for ATTR patients (3–5 years) but high morbidity and mortality is associated with both forms of the disease [4, 5].

Cardiac $ATTR_{wt}$ amyloidosis is thought to be common among elderly patients who have heart failure with preserved ejection fraction [6]. Indeed, a population-based autopsy study revealed the presence of cardiac ATTR amyloid deposits in up to 25% of individuals over 85 years of age [7]. A major diagnostic challenge is that symptoms do not develop until a substantial quantity of amyloid has accumulated. Moreover, symptoms are non-specific and awareness of amyloidosis is limited, frequently leading to a very delayed or missed diagnosis.

The traditional gold standard for diagnosis of cardiac ATTR amyloid deposits is Congo red staining of myocardial biopsies which exhibit pathognomonic green birefringence when viewed under crossed-polarised light [8]. Amyloid type can then be sought with immunohistochemical staining using a panel of antibodies to specific amyloid fibril proteins. Hereditary aetiologies are determined by the presence of gene mutations. However, endomyocardial biopsy, which should be taken from the left

ventricle, is associated with a small but not insignificant risk of fatal complications and the requirement for specific expertise introduces diagnostic delay [9, 10].

Optimal clinical management requires detection and correct identification of amyloid fibril type to avoid misdiagnosis and inappropriate toxic treatment [11, 12]. Current therapeutic options are focused on efforts to reduce supply of the respective amyloid fibril precursor protein [13]. Treatment of AL comprises chemotherapy to target the underlying plasma cell dyscrasia and hence suppress production of amyloidogenic light chain proteins. Crucially, chemotherapy has no role in the treatment of ATTR amyloidosis, emphasising the importance of correct diagnoses.

The role of imaging

Echocardiography is a valuable and widely accessible tool that can identify significant abnormalities in patients with heart failure, such as left-ventricular-wall thickening but is neither specific nor sensitive for cardiac amyloidosis [14]. Gadolinium-enhanced cardiovascular magnetic resonance imaging (CMR) can identify myocardial infiltration and plays an important role in the diagnosis and prognosis of cardiac amyloidosis [14]. However, false negatives can occur, it is often only implemented in specialist centres, and it is contraindicated in a substantial proportion of patients [15–17].

Nuclear medicine imaging facilitates diagnoses and interventions by visualising amyloid deposits. ^{123}I-labelled serum amyloid P component (^{123}I-SAP), which binds to all types of amyloid fibril, is used for diagnosing, locating, and monitoring the extent of systemic amyloidosis [18, 19]. ^{123}I-SAP scintigraphy cannot, however, detect the presence of amyloid in affected myocardial areas due to the low permeability of ^{123}I-SAP in cardiac tissue and relatively-high blood pool background [20].

Radiolabelled phosphate derivatives, developed as bone-seeking radiotracers for skeletal scintigraphy, were noted to bind to amyloid deposits over 40 years ago but there has been much delay in developing bone tracers for this new indication since 1981 [21–23]. Although none are yet licensed for imaging cardiac amyloidosis, there is robust evidence showing that imaging with ^{99m}Tc-labelled 3,3-diphosphono-1,2-propanodicarboxylic acid (DPD), pyrophosphate (PYP), and hydroxymethylene diphosphonate (HMDP) possesses enormous diagnostic value in patients with cardiac ATTR amyloidosis [24–28].

^{99m}Tc-DPD scintigraphy has shown particular promise in evaluating cardiac amyloidosis [29]. Gillmore *et al* recently confirmed that it has remarkable diagnostic sensitivity and specificity for ATTR

amyloidosis when implemented as part of a simple clinical algorithm [30]. At the UK National Amyloidosis Centre (NAC) ^{99m}Tc-DPD scintigraphy has been routinely carried out on all patients with suspected or histologically proven cardiac amyloidosis to support or exclude diagnoses of cardiac ATTR amyloidosis and to monitor disease extent since June 2010.

Quantitative imaging

Quantitation, in principle, offers the potential to support visual interpretation of cardiac amyloidosis with an objective measure of amyloid burden. The capability to generate accurate quantitative data would also better enable interval monitoring of disease progression or response to treatment. In addition, numerical thresholds could be developed to support or exclude diagnoses for patients with non-specific symptoms or patients undergoing screening investigations or skeletal scintigraphy. The prognostic implications of greater radiotracer uptake in the myocardium, expressed as mortality and morbidity, could be investigated too.

The aim of this study was to investigating the feasibility and utility of estimating ^{99m}Tc-DPD uptake in myocardial tissue; this has the potential to yield reliable quantitative information on cardiac amyloid burden, which is urgently required to monitor disease progression and response to novel treatments.

Materials and methods

Patients

Seventy-four patients with confirmed cardiac ATTR amyloidosis were referred to the NAC for further evaluation and underwent ^{99m}Tc-DPD scintigraphy investigations between July 2010 and August 2016. Together they formed a cohort of patients on whom at least three investigations were performed as part of an ongoing longitudinal study of cardiac ATTR amyloid burden progression over time. Only baseline image data were analysed for the purposes of this investigation. Within this cohort there were 45 patients with $ATTR_{wt}$ and 29 patients with $ATTR_{mt}$, associated with genetic TTR mutations V122I (n = 9), T60A (n = 9), G47V (n = 3), E54G (n = 2), V30M (n = 2), E89K (n = 1), F44L (n = 1), I107F (n = 1), or I84S (n = 1).

Acquisitions

Images were acquired with two General Electric (GE) hybrid SPECT-CT gamma cameras (GE Healthcare, Chicago, IL, USA): namely, an Infinia Hawkeye 4 and a Discovery NM/CT 670. Patients were intravenously administered with approximately 700 MBq (18.9 mCi) of ^{99m}Tc-DPD (Teceos®, CIS Bio International, Gif-sur-Yvette, France), equating to an estimated effective dose of 5.6 mSv. A protocol consisting of a planar whole-body acquisition followed immediately by cardiac SPECT with low-energy, high-resolution collimators and non-contrast CT for the purposes of attenuation correction and anatomical localisation was initiated subsequent to radiotracer administration with a median delay (Q_1, Q_3) of 2:57 (2:49, 3:10) hours. Anterior and posterior whole-body images were acquired onto 256 × 1024 matrices at a speed of 10 cm/min with the patient in the supine position. SPECT data were reconstructed onto 256 × 256 matrices with an ordered-subset expectation maximisation (OSEM) algorithm (6i10s) on a GE Xeleris workstation following scatter correction and collimator-detector response compensation with Resolution Recovery. Counts were recorded and decay-corrected and the amount of radioactivity and the sensitivities of both gamma cameras were accounted for in each method. In the case of extravasation the amount of activity at the injection site was estimated and deducted from the dose administered.

Perugini grade

Cardiac involvement in ^{99m}Tc-DPD images was reported by experienced clinicians, who scored uptake with grades from a modified version of the Perugini grading system: grade 0 (cardiac uptake not visible in either planar whole-body or fused SPECT-CT images), grade 1 (cardiac uptake visible only in SPECT-CT images and/or mild cardiac uptake visible but inferior to skeletal uptake in planar whole-body images), grade 2 (moderate cardiac uptake visible, equal to or greater than skeletal uptake, in planar whole-body images), or grade 3 (strong cardiac uptake visible in conjunction with little or no evident skeletal signal in planar whole-body images) [24].

Quantitation

Three different methods of quantitation were used for this investigation. Each technique was carried out by an experienced nuclear medicine technologist. One approach used data from the planar whole-body images (1), whilst the remaining two used data from the SPECT-CT images (2 and 3). The areas of analysis were the whole heart in planar images and the left-ventricular myocardium and the entire

volume of the heart in SPECT images. Correlations between the resultant datasets were assessed to corroborate findings and assess reliability. They were also compared to the results of an independent method (4) as a form of validation. The quantitative results of each method were compared to the grades reported by an experienced clinician to investigate how these grades relate to the amount ^{99m}Tc-DPD uptake.

1. Heart to contralateral

This approach was developed for whole-body ^{99m}Tc-PYP imaging by colleagues in the U.S [27]. A circular region of interest (ROI) is drawn over the heart and copied and mirrored to the contralateral chest to enable the 'heart-to-contralateral ratio' (H/CL) to be calculated from the quotient of the two. Results here were generated on Xeleris v.3.1 (GE Healthcare, Chicago, IL, USA) on a Xeleris workstation.

2. Left ventricle

Cardiac ATTR amyloidosis, particularly $ATTR_{wt}$, is associated with increased left-ventricular-wall thickness. Thus, for this investigation, ^{99m}Tc-DPD uptake in this region was hypothesised as a surrogate for total radiotracer uptake across the whole heart in SPECT-CT images [31].

A custom method of quantifying ^{99m}Tc-DPD uptake was developed: SPECT data were analysed using an in-house plugin of OsiriX v.9.0 (OsiriX Foundation, Switzerland), an open-source application for viewing and processing DICOM (Digital Imaging and Communications in Medicine) images [32]. The centre of ^{99m}Tc-DPD uptake was manually delineated along the short axis of the myocardium using three one-voxel-thick regions at the base, middle, and apex of the heart (Fig. 1). From these sampling regions a 16-segment dataset was extracted, where uptake was expressed in counts [33]. The method was validated against a similar approach (supplementary data have been supplied).

3. Whole heart

Absolute uptake throughout the heart was assessed using Q.Metrix (GE Healthcare, Chicago, IL, USA), which was available on a Xeleris workstation. Q.Metrix utilises CT and SPECT segmentation tools. For each patient the heart was outlined according to CT image data to produce an individual ROI on each

slice prior to generating a volume of interest (VOI) for the whole heart. This VOI was then copied to the SPECT dataset for quantitation. Final results were expressed as percentages of injected doses.

4. Extracellular volume

Strong correlations between all of the ^{99m}Tc-DPD scintigraphy dataset pairs would not imply that each approach accurately quantified amyloid burden independently: it would only suggest that we can be more confident in the results of a single method with respect to their collective interpretation. Therefore correlations were assessed between quantitative ^{99m}Tc-DPD scintigraphy data and the results of an independent method: namely, the measurement of extracellular volume fraction (ECV) by CMR, whereby extracellular volume expansion is indicative of the presence of cardiac amyloid. Forty-four of the 74 patients underwent CMR acquisitions within six months of ^{99m}Tc-DPD acquisitions; the remainder of patients were contraindicated for CMR or their acquisitions were performed outside of this time window, which was applied to minimise the impact of disease change on the analysis ECV results were separated by Perugini grade to investigate how ECV expansion relates to Perugini grade. Correlations between ECV and quantitative ^{99m}Tc-DPD scintigraphy results were assessed to gain an understanding of any underlying relationships.

Statistics

The datasets were analysed on IBM SPSS Statistics 25 software. Following assessments of normality Mann-Whitney *U* tests were used to determine whether differences between datasets separated by Perugini grade were statistically significant. Linear relationships between ^{99m}Tc-DPD uptake and ECV data were hypothesised. Correlations were quantified with Pearson correlation coefficients and expressed as coefficients of determination, R^2, to evaluate goodness of fit of linear regression lines.

Results

Cardiac involvement was graded as 1 (n = 15), 2 (n = 39), or 3 (n = 20).

Coefficients of determination, representing correlations between dataset pairs, are listed in Table 1. A strong correlation was observed in each case, suggesting that all three measures convey comparable information with regard to ^{99m}Tc-DPD uptake.

The quantitative results generated with each method were separated by Perugini grade (Fig. 2). A consistent pattern emerged: the grade-2 and grade-3 distributions were significantly greater than the grade-1 distributions; however, none of the grade 3 distributions were significantly greater than the grade-2 distributions. For the planar results the grade-3 distribution was significantly smaller than the grade-2 distribution. In contrast to all of the relationships above, the median ECV was significantly higher for the grade-3 distribution than it was for the grade-2 patient distribution, as shown in Fig. 3.

Linear relationships between ^{99m}Tc-DPD uptake and ECV datasets were evaluated with Pearson correlation coefficients. Each assessment demonstrated a strong linear correlation. However, heteroscedasticity was observed for high ECV values, which implies that linearity between ^{99m}Tc-DPD uptake and ECV eventually breaks down. Spearman correlation coefficients, ρ, were, therefore, generated to evaluate monotonic relationships. Both statistical parameters suggest that ^{99m}Tc-DPD uptake is expected to be greater when ECV is greater ($p < 0.001$). The relationship between percentage of injected dose and ECV and the statistical results are shown in Fig. 4.

Uptake within the left ventricle was regionalised using OsiriX (Fig. 5). The most significant difference was observed between uptake in the septal wall and lateral wall of the left ventricle. A significant difference between uptake in the base and the apex was also observed.

Discussion

To the best of our knowledge, no other study to date has investigated multiple techniques of quantitation of myocardial ^{99m}Tc-DPD uptake for patients with cardiac ATTR amyloidosis. We hoped to gain an understanding of how quantitative results should be interpreted if we are to accurately measure cardiac amyloid burdens with them.

Three different approaches were used to examine radiotracer uptake in myocardial tissue in 74 patients. We separated the results by Perugini grade, assessed correlations between datasets, and compared the datasets to the results of an independent method. We also regionalised ^{99m}Tc-DPD uptake in the myocardia of patients' left ventricles to gain a greater insight into ^{99m}Tc-DPD uptake patterns.

The strong correlations we found suggest that any of the investigated techniques could be employed to quantitatively assess ^{99m}Tc-DPD uptake in ATTR-positive patients. However, although all of the quantitative approaches may yield similar clinical interpretations to each other in the future, their

results will not necessarily correlate with the amount of amyloid because the relationship between radiotracer uptake and burden of cardiac amyloid is still not clear.

Results reported here show that grade-1 patients were, on average, distinguishable from grade-2 and grade-3 patients in terms of ^{99m}Tc-DPD uptake. However, median uptake in grade-3 patients was either not statistically different to uptake in grade-2 patients or it was significantly less. Thus, on the basis of our results, the postulation of the Perugini grading system that higher grades represent greater cardiac uptake is false. Hence Perugini grades, contrary to their classifications, do not translate to meaningful quantitative information across a wide range of uptake patterns.

The Perugini approach is subjective for patients with borderline uptake patterns. Further, the grades do not necessarily convey prognostic information: it has been demonstrated that survival outcomes between patients whose cardiac uptake patterns have been assigned grade 1, grade 2, and grade 3 do not differ; and, once diagnosed, all of these patients follow the same treatment pathway [30, 34]. There is, therefore, a need to question its clinical utility, especially for differentiating grade-2 and grade-3 patients. It is the presence of cardiac amyloid indicated by abnormal ^{99m}Tc-DPD uptake in the heart rather than Perugini grade of uptake that confers prognostic significance for patients with ATTR amyloidosis [34].

Our previous findings showed that amyloid deposition in extra-cardiac skeletal muscle gives rise to three-compartmental competition for radiotracer between bone and amyloid in myocardial tissue and amyloid in skeletal muscle [34, 35]. Through this latest study we present evidence of this phenomenon interfering with the interpretation of cardiac amyloid burden from ^{99m}Tc-DPD uptake. If amyloid deposition in extra-cardiac soft tissue is substantial, it would follow that some patients with larger cardiac amyloid burdens would have less ^{99m}Tc-DPD uptake in myocardial tissue than patients with lower cardiac burdens in whom skeletal muscle amyloid was less pronounced. This seemingly-insurmountable phenomenon may well have implications for serial studies in individual patients, who may have progressive skeletal muscle involvement during study intervals.

A supplementary technique which was not investigated here is the calculation of radiotracer retention values, which a number of other groups utilise. Perugini *et al* posed that ATTR patients, AL patients, and controls can be differentiated by calculating ^{99m}Tc-DPD retention between acquisitions at 5 minutes (early) and 3 hours (late) after administration [24]. Further, another group demonstrated that a H/WB value greater than 7.5 was a significant predictor of survival for patients who had not

experienced major adverse cardiovascular events [29]. However, as it stands, early imaging is not performed at the NAC because, for the added scanning time, it is not deemed to add diagnostic value to our current clinical algorithm [30]. We, therefore, could not investigate retention as a quantitative parameter, which we accept as a shortfall of this investigation.

We did investigate one planar-based metric, H/CL, which was simple and versatile. Frequently, however, it was necessary to alter the ROIs to avoid inclusion of counts from underlying and overlying anatomical structures, including the sternum, liver, ribs, and spine. Moreover, despite the lack of published guidelines, it is known that lung uptake can be present in a substantial proportion of patients, a phenomenon that would also contribute unwanted counts to ROIs that cannot be differentiated from counts originating in myocardial tissue (Fig. 6) [36]. There is a chance that this caused H/CL to be a spuriously-low surrogate of cardiac amyloid burden in some high-grade patients. Another fundamental disadvantage to quantifying ^{99m}Tc-DPD uptake in planar images which reduces quantitative accuracy is the lack of a reliable method of attenuation correction.

Our SPECT-based methods circumvented the issues associated with two-dimensional imaging. Radiotracer uptake is visualised in three dimensions; theoretically, then, SPECT-CT can play a role in highlighting the location and characteristics of radiotracer uptake with improved accuracy and precision. We demonstrated that quantitation of ^{99m}Tc-DPD SPECT data of the left ventricle was a good surrogate of total cardiac uptake despite being measured with a one-voxel-thick sampling region. We also showed that ^{99m}Tc-DPD uptake, which is regularly non-uniform across myocardial tissue, was more likely to be found in septal and basal regions than in lateral and apical regions. Another benefit was that CT data could be utilised for visualising cardiac boundaries for the purposes of outlining. Nonetheless, our quantitative planar results correlated strongly with the quantitative SPECT and ECV results. As such, the added value of SPECT was lower than expected.

Similarly to radiotracer retention, a benefit of adopting H/CL would be that it has already been shown to convey valuable prognostic information, where H/CLs greater than 1.6 were associated with poorer survival outcomes [37]. However, the authors of this particular study demonstrated that, in a population of patients with advanced ATTR amyloidosis, ^{99m}Tc-PYP uptake did not alter despite evidence of marked disease progression. This suggests that this method is insensitive to changes in radiotracer uptake or that uptake does not correlate with disease extent for high-grade uptake. Either conclusion would render the technique, like our other, SPECT-based approaches, inappropriate for

repeat quantitative studies, where changes in uptake must be confidently assumed to match changes in cardiac amyloid burden.

Assuming that greater ECV is indicative of greater amyloid deposition, our strong correlation coefficients would suggest that there is a strong association between ^{99m}Tc-DPD uptake in the heart and cardiac amyloid burden. But since ECV is not a proven gold standard and since correlation does not imply causation, it would be naïve to assume this across a wide range of cardiac involvement, for strong correlations between ^{99m}Tc-DPD uptake and ECV might be attributable to a cause which is different to amyloid deposition. Furthermore, the correlations deteriorated with Perugini grade: grade-3 patients, on average, presented with significantly greater ECV than grade-2 patients but the equivalent was not true for ^{99m}Tc-DPD uptake.

Future

The molecular basis of the ^{99m}Tc-DPD binding mechanism to amyloid fibrils remains unknown. Our understanding is further hampered by the fact that its uptake patterns, like any tracer, are dynamic in nature. The interdependence of three compartments—bone, myocardial tissue, and soft tissue—presents a major challenge to quantifying uptake in any particular site, regardless of whether quantitation is performed on planar or SPECT data. The inability to accurately measure cardiac amyloid burden with ^{99m}Tc-DPD scintigraphy for high-grade patients is a major issue with respect to predicting prognostic outcomes of patients diagnosed with cardiac ATTR amyloidosis.

However, this should not dissuade other groups from investigating the utility of quantitation for low-grade patients. A follow-on project subsequent to this study might entail undertaking one or more of the following: a technical investigation similar to ours where patients who exhibit a greater range of amyloid burdens are recruited over a longer period of time to further our understanding of how the disease develops in its early stages and to minimise the likelihood of selection bias; an attempt to reliably express quantitative values as predictors of morbidity and survival, already explored to an extent for retention and H/CL with planar data; or a mechanistic study of ^{99m}Tc-DPD uptake, where radiotracer kinetics are studied in detail and quantitative results are corroborated with other biomarkers to further our understanding of what uptake actually implies [29, 37]. Although interobserver variability was not an issue by virtue of there being one person drawing regions, any future study should better attempt to

account for both interobserver and intraobserver variability by recruiting more observers and by commenting on differences between their results.

Conclusions

We developed and tested three approaches to quantitation of ^{99m}Tc-DPD uptake in myocardial tissue to assess its relationship with cardiac amyloid burden. Quantitation of ^{99m}Tc-DPD uptake in cardiac transthyretin amyloid deposits is complex and is hindered by competition for radiotracer with amyloid in skeletal muscle. The latter underlies differences in uptake between grade-2 and grade-3 patients, not cardiac uptake.

Notes

Acknowledgements

JCR, DFH, MB, and JP were responsible for data collection and analysis; JAS for development of the in-house OsiriX plugin used; and JDG, ADW, PNH, and MF for interpretation of results and critical review of the manuscript.

Funding

GE Healthcare provided a trial licence for the use of Q.Metrix.

Compliance with ethical standards

Conflicts of interest

None.

Ethical approval

All procedures performed in studies involving human participants were in accordance with the ethical standards of the institutional and/or national research committee and with the principles of the 1964 Declaration of Helsinki and its later amendments or comparable ethical standards.

Informed consent

For this type of study formal consent is not required.

References

[1] Lachmann HJ, Hawkins PN. Systemic amyloidosis. *Curr Opin Pharmacol* 2006; **6**: 214–220.

[2] Sipe JD, Benson MD, Buxbaum JD, Ikeda S, Merlini G, Saraiva MJ, *et al*. Nomenclature 2014: Amyloid fibril proteins and clinical classification of the amyloidosis. *Amyloid* 2014; **21**: 221–224.

[3] Benson MD. The hereditary amyloidoses. *Best Pract Res Clin Rheumatol* 2003; **17**: 909–927.

[4] Dubrey SW, Cha K, Anderson J, Chamarthi B, Reisinger J, Skinner M, *et al*. The clinical features of immunoglobulin light-chain (AL) amyloidosis with heart involvement. *QJM* 1998; **91**: 141–57.

[5] Dungu JN, Anderson LJ, Whelan CJ, Hawkins PN. Cardiac transthyretin amyloidosis. *Heart* 2012; **98**: 1546–1554.

[6] Mirzoyev SA, Edwards WD, Mohammed SF, Donovan JL, Roger VL, Grogan DR, *et al*. Cardiac amyloid deposition is common in elderly patients with heart failure and preserved ejection fraction. *Circulation* 2010; **122**: A17926.

[7] Tanskanen M, Peuralinna T, Polvikoski T, Notkola I-L, Sulkava R, Hardy J, *et al.* Senile systemic amyloidosis affects 25% of the very aged and associates with genetic variation in alpha2-macroglobulin and tau: a population-based autopsy study. *Ann Med* 2008; **40**: 232–239.

[8] Puchtler H, Sweat F, Levine M. On the binding of Congo red by amyloid. *J Histochem Cytochem* 1962; **10**: 355–364.

[9] Fine NM, Arruda-Olson AM, Dispenzieri A, Zeldenrust SR, Gertz MA, Kyle RA. Yield of noncardiac biopsy for the diagnosis of transthyretin cardiac amyloidosis. Am J Cardiol. 2014; **113:** 1723–1177.

[10] Maurer MS. Noninvasive identification of ATTRwt cardiac amyloid: the re-emergence of nuclear cardiology. *Am J Med* 2015; **128**: 1275–1280.

[11] Lachmann HJ, Booth DR, Booth SE, Bybee A, Gilbertson JA, Gillmore JD, *et al*. Misdiagnosis of hereditary amyloidosis as AL (primary) amyloidosis. *N Engl J Med* 2002; **346**: 1786-1791.

[12] Sachchithanantham S, Wechalekar AD. Imaging in systemic amyloidosis. *Br Med Bull* 2013; **107**: 41–56.

[13] Wechalekar AD, Gillmore JD, Hawkins PN. Systemic amyloidosis. *Lancet* 2016; **387**: 2641–2654.

[14] Falk RH. Diagnosis and management of the cardiac amyloidoses. *Circulation* 2005; **112**: 2047–2060.

[15] Fontana M, Pica S, Reant P, Abdel-Gadir A, Treibel TA, Banypersad SM, *et al*. Prognostic value of late gadolinium enhancement cardiovascular magnetic resonance in cardiac amyloidosis. *Circulation* 2015; **132**: 1570–1579.

[16] Austin BA, Tang WHW, Rodriguez ER, Tan C, Flamm SD, Taylor DO, *et al*. Delayed hyper-enhancement magnetic resonance imaging provides incremental diagnostic and prognostic utility in suspected cardiac amyloidosis. *JACC Cardiovascular imaging* 2009; **2**: 1369–1377.

[17] Dungu JN, Valencia O, Pinney JH, Gibbs SD, Rowczenio D, Gilbertson JA, *et al*. CMR-based differentiation of AL and ATTR amyloidosis. *JACC Cardiovasc Imaging* 2014; **7**: 133–142.

[18] Hawkins PN, Lavender JP, Pepys MB. Evaluation of systemic amyloidosis by scintigraphy with ^{123}I-labeled serum amyloid P component. *The New England journal of medicine* 1990; **323**: 508–513.

[19] Hawkins P. Serum amyloid P component scintigraphy for diagnosis and monitoring amyloidosis. *Curr Opin Nephrol Hypertens* 2002; **11**: 649–655.

[20] Glaudemans AWJM, Slart RHJA, Zeebregts CJ, Veltman NC, Tio RA, Hazenberg BPC, *et al*. Nuclear imaging in cardiac amyloidosis. *Eur J Nucl Med Mol Imaging* 2009; **36**: 702–714.

[21] VanAntwerp JD, O'Mara RE, Pitt MJ, Walsh S. Technetium-99m-diphosphonate accumulation in amyloid. *J Nucl Med* 1975; **16**: 238–240.

[22] Ali A, Turner DA, Rosenbush SW, Fordham EW. Bone scintigram in cardiac amyloidosis: a case report. *Clin Nucl Med* 1981; **6**: 105–108.

[23] Bokhari S, Shahzad R, Castaño A, Maurer MS. Nuclear imaging modalities for cardiac amyloidosis. *J Nucl Cardiol* 2014; **21**: 175–184.

[24] Perugini E, Guidalotti PL, Salvi F, Cooke RM, Pettinato C, Riva L, *et al*. Noninvasive etiologic diagnosis of cardiac amyloidosis using ^{99m}Tc-3,3-diphosphono-1,2-propanodicarboxylic acid scintigraphy. *J Am Coll Cardiol* 2005; **46**: 1076–1084.

[25] Rapezzi C, Guidalotti P, Salvi F, Riva L, Perugini E. Usefulness of ^{99m}Tc-DPD scintigraphy in cardiac amyloidosis. *J Am Coll Cardiol* 2008; **51**: 1509–1510

[26] Rapezzi C, Quarta CC, Guidalotti PL, Longhi S, Pettinato C, Leone O, *et al*. Usefulness and limitations of ^{99m}Tc-3,3-diphosphono-1,2-propanodicarboxylic acid scintigraphy in the aetiological diagnosis of amyloidotic cardiomyopathy. *Eur J Nucl Med Mol Imaging* 2011; **38**: 470–478.

[27] Bokhari S, Castaño A, Pozniakoff T, Deslisle S, Latif F, Maurer MS. ^{99m}Tc-Pyrophosphate Scintigraphy for Differentiating Light-Chain Cardiac Amyloidosis From the Transthyretin-Related Familial and Senile Cardiac Amyloidoses. *Circ Cardiovasc Imaging* 2013; **6**: 195–201.

[28] Quarta CC, Guidalotti PL, Longhi S, Pettinato C, Leone O, Ferlini A, *et al*. Defining the diagnosis in echocardiographically suspected senile systemic amyloidosis. *JACC Cardiovasc Imaging* 2012; **5**: 755–758.

[29] Rapezzi C, Quarta CC, Guidalotti PL, Pettinato C, Fanti S, Leone O, *et al*. Role of ^{99m}Tc-DPD scintigraphy in diagnosis and prognosis of hereditary transthyretin-related cardiac amyloidosis. *JACC Cardiovasc Imaging* 2011; **4**: 659–670.

[30] Gillmore JD, Maurer MS, Falk RH, Merlini G, Damy T, Dispenzieri A, *et al*. Non-biopsy diagnosis of cardiac transthyretin amyloidosis. *Circulation* 2016; **133**: 2404–2412.

[31] Gertz MA, Benson MD, Dyck PJ, Grogan M, Coelho T, Cruz M, *et al*. Diagnosis, Prognosis, and Therapy of Transthyretin Amyloidosis. *J Am Coll Cardiol* 2015; **66**: 2451–2466.

[32] Rosset A, Spadola L, Ratib O. OsiriX: An Open-Source Software for Navigating in Multidimensional DICOM Images. *J Digit Imaging* 2004; **17**: 205–216.

[33] Cerqueira MD, Weissman NJ, Dilsizian V, Jacobs AK, Verani MS, Kaul S, *et al*. the Heart: A Statement for Healthcare Professionals From the Cardiac Imaging Standardized Myocardial Segmentation and Nomenclature for Tomographic Imaging of Committee of the Council on Clinical Cardiology of the American Heart Association. *Circulation* 2002; **105**: 539–542

[34] Hutt DF, Fontana M, Burniston M, Quigley A-M, Petrie A, Ross JC, *et al*. Prognostic utility of the Perugini grading of ^{99m}Tc-DPD scintigraphy in transthyretin (ATTR) amyloidosis and its relationship with skeletal muscle and soft tissue amyloid. *Eur Heart J Cardiovasc Imaging* 2017; **0**: 1–7.

[35] Hutt DF, Quigley A-M, Page J, Hall ML, Burniston M, Gopaul D, *et al*. Utility and limitations of 3,3-diphosphono-1,2-propanodicarboxylic acid scintigraphy in systemic amyloidosis. Eur Heart J Cardiovasc Imaging 2014; **15**: 1289–1298.

[36] Cappelli F, Gallini C, Costanzo EN, Tutino F, Ciaccio A, Vaggelli L *et al*. Lung uptake during 99mTc-hydroxymethylene diphosphonate scintigraphy in patient with TTR cardiac amyloidosis: An underestimated phenomenon. *Int J Cardiol* 2018; **254**: 346–350.

[37] Castaño A, DeLuca A, Weinberg R, Pozniakoff T, Blaner WS, Pirmohamed A, *et al*. Serial scanning with technetium pyrophosphate (^{99m}Tc-PYP) in advanced ATTR cardiac amyloidosis. *J Nucl Cardiol* 2016; **23**: 1355–1363.

Supplementary data

Myovation™ (GE Healthcare, Chicago, IL, USA), a dedicated cardiac application for Xeleris workstations, was employed to quantify ^{99m}Tc-DPD uptake in the myocardial tissue of left ventricles for

the same cohort of patients. The resultant data was used to validate the results generated with OsiriX and its particular method of outlining uptake in the left ventricle.

For each patient an experienced nuclear medicine technologist defined the axes of the heart in Myovation™, which then determined the centre of uptake along the short axis of the heart automatically. Unlike OsiriX, Myovation™ generates a 17-segment parametric polar map of radiotracer uptake, which incorporates the tip of the apex in the 17th segment. As with OsiriX, sampling regions were one-voxel thick.

Although a strong correlation between the results of both methods was found ($p < 0.001$), in 27 cases (12.6 %), representing the images of ten grade-1 patients (13.5 %), the Myovation™ approach to quantifying uptake in the left ventricle could not process the data due to insufficient numbers of counts. The OsiriX method did not suffer from this drawback as it benefitted from manual drawing tools. However, despite both techniques measuring counts from the same anatomical region, the OsiriX method consistently produced results smaller than the Myovation™ method, as shown in Fig. 7.

Spatial resolution of SPECT images is an important factor in the context of precise quantitation (Fig. 8). The bias observed between the two datasets may be due to differences in interpolation settings, which could be altered in OsiriX but were unknown and unalterable in Myovation™.

Thus the OsiriX approach was considered superior for quantifying radiotracer uptake in the left ventricle.

Captions, figures, and tables

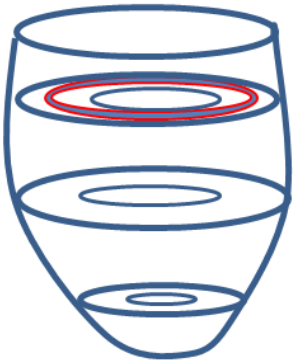

Fig. 1: Delineation of ^{99m}Tc-DPD uptake in the left-ventricular base of the myocardium is diagrammatically presented.

Parameters (*n*)	R^2 (*p*)
H/CL (74) and OsiriX (74)	0.646 (< 0.001)
H/CL (74) and Q.Metrix (74)	0.619 (< 0.001)
OsiriX (74) and Q.Metrix (74)	0.637 (< 0.001)

Table 1: Coefficients of determination and statistical significance.

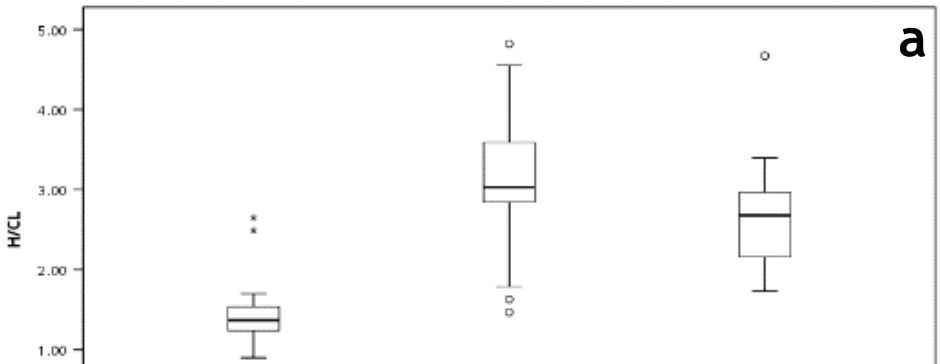

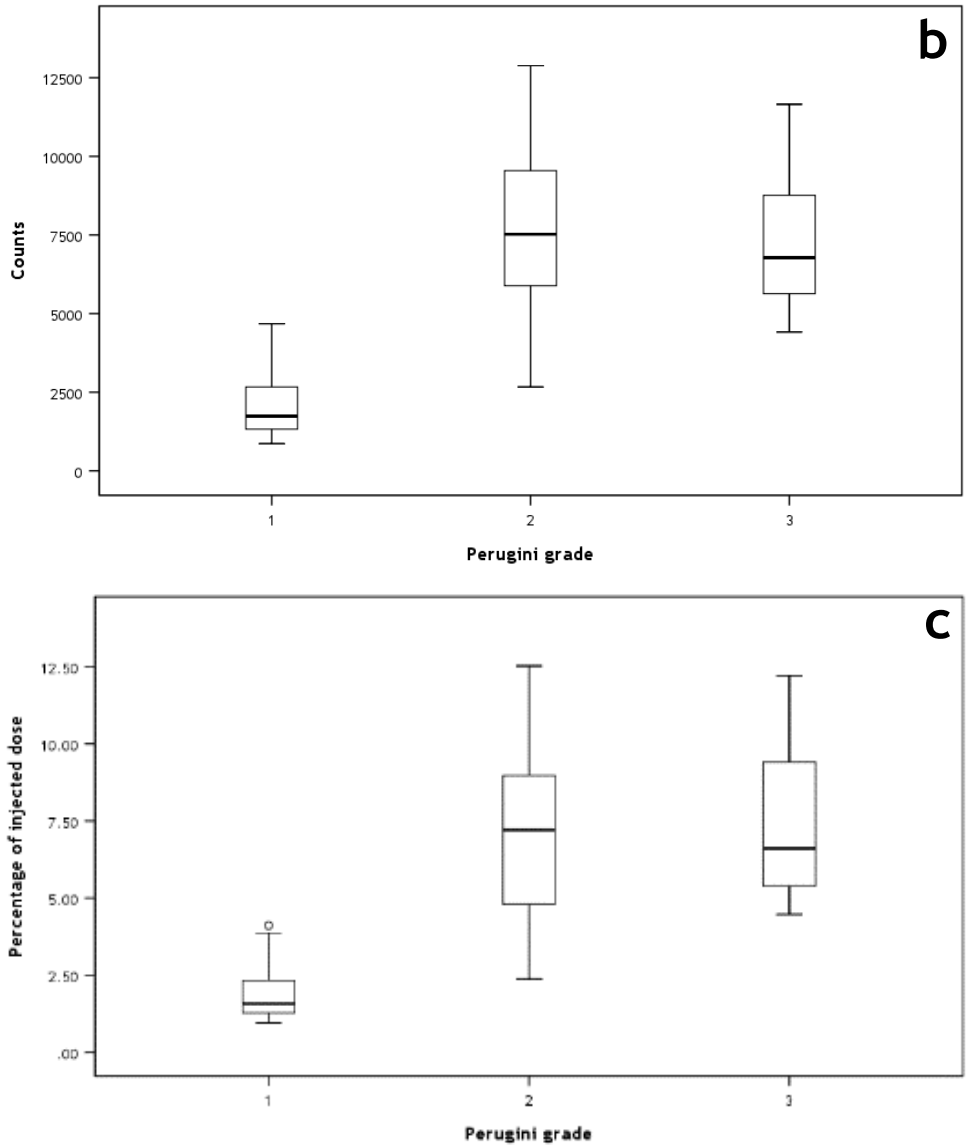

Fig. 2: Results separated by Perugini grade for (a) H/CL, (b) OsiriX, and (c) Q.Metrix. *p* values representing the statistical significance of differences (grade 1 *vs* grade 2; grade 2 *vs* grade 3) were as follows: H/CL (< 0.001; 0.01), OsiriX (< 0.001; 0.35), and Q.Metrix (< 0.001; 0.60).

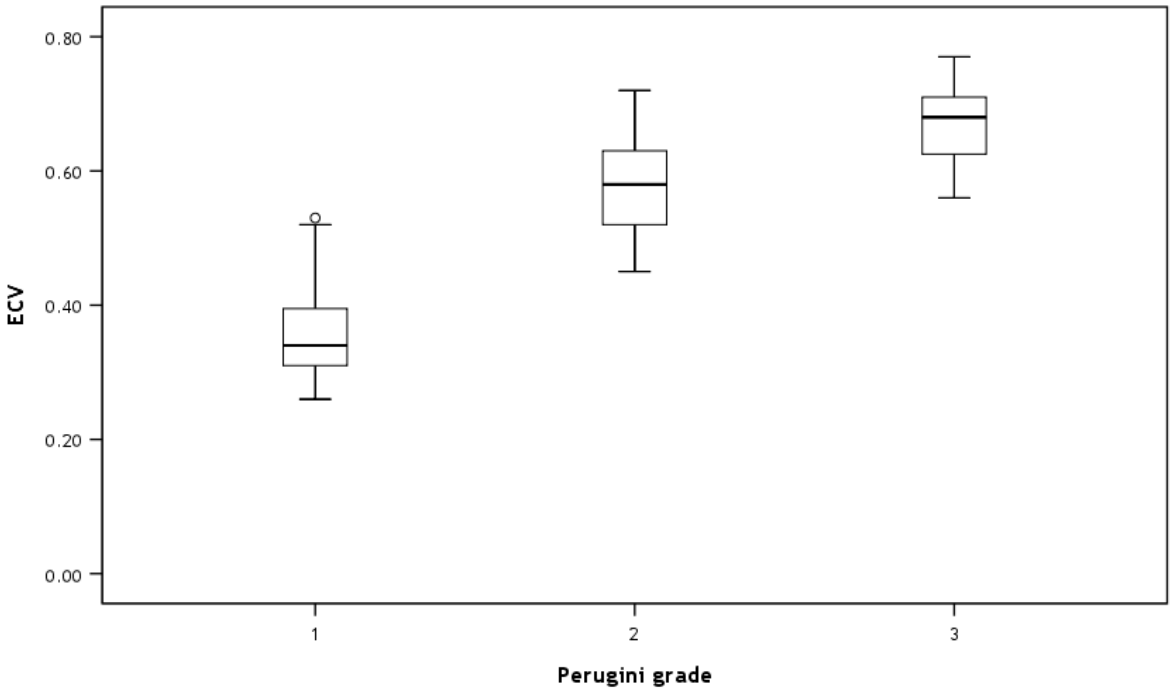

Fig. 3: ECV results separated by Perugini grade. *p* values for the comparisons of the grade 1 and grade 2 distributions and the grade 2 and grade 3 distributions were $p < 0.001$ and 0.01 respectively.

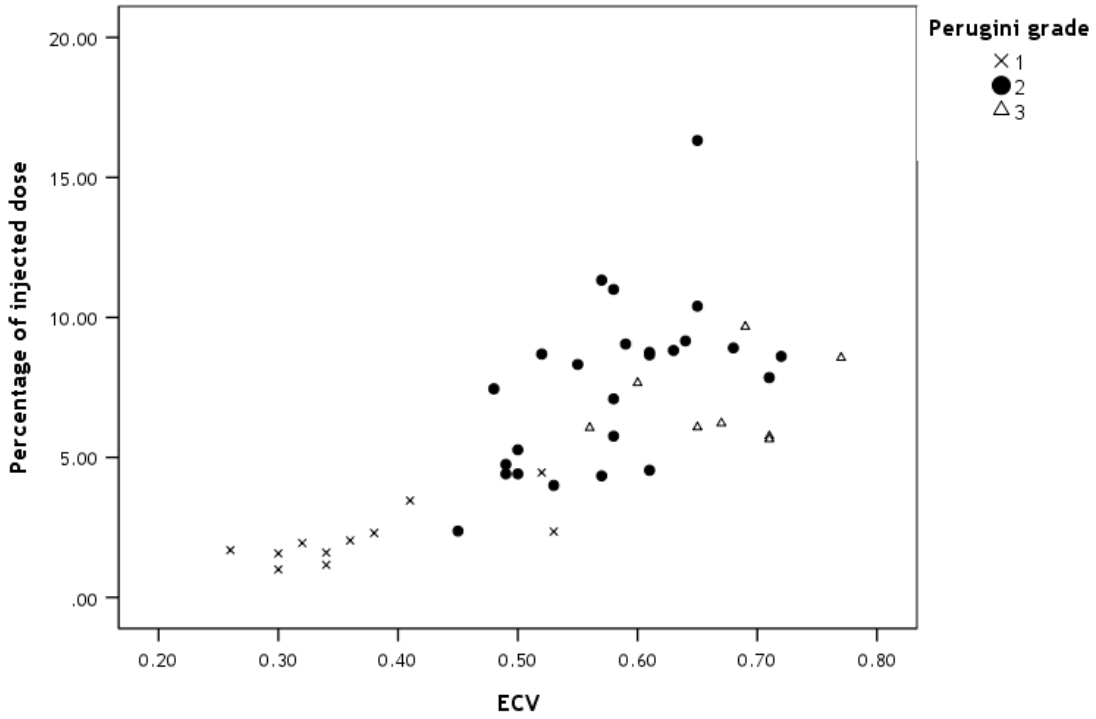

Fig. 4: Percentage of injected dose results plotted against ECV results. Correlation (R^2, *p*; ρ, *p*) with ECV was strong for H/CL (0.27, $p < 0.001$; 0.21, $p < 0.001$), OsiriX (0.55, $p < 0.001$; 0.48, $p < 0.001$), and Q.Metrix (0.53, $p < 0.001$; 0.54, $p < 0.001$).

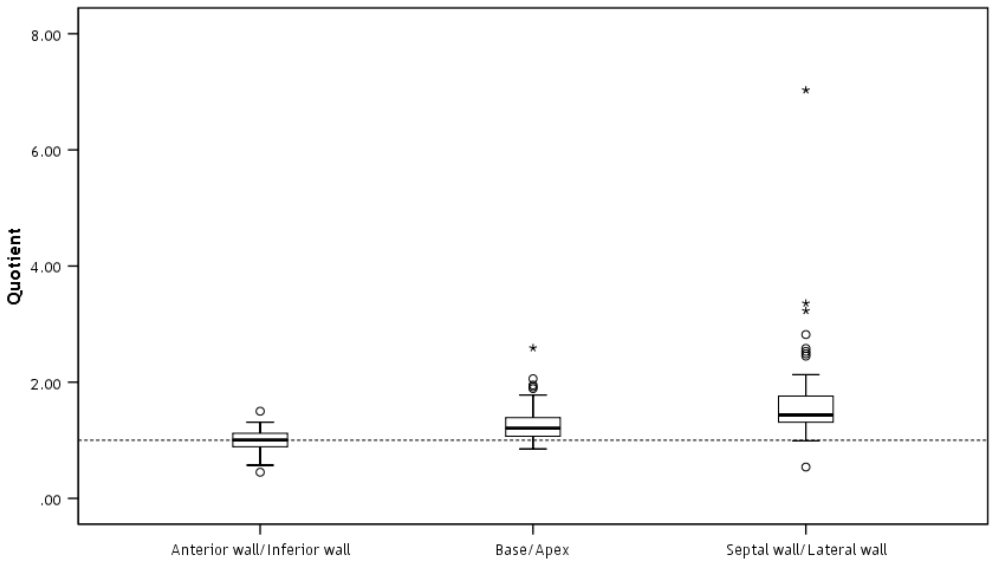

Fig. 5: The quotients of uptake in different regions of the left-ventricular myocardium as regionalised with OsiriX. Significant differences were observed between septal wall and lateral wall ($p < 0.001$) and the base and apex ($p = 0.02$) but not between the anterior wall and inferior wall ($p = 1.00$).

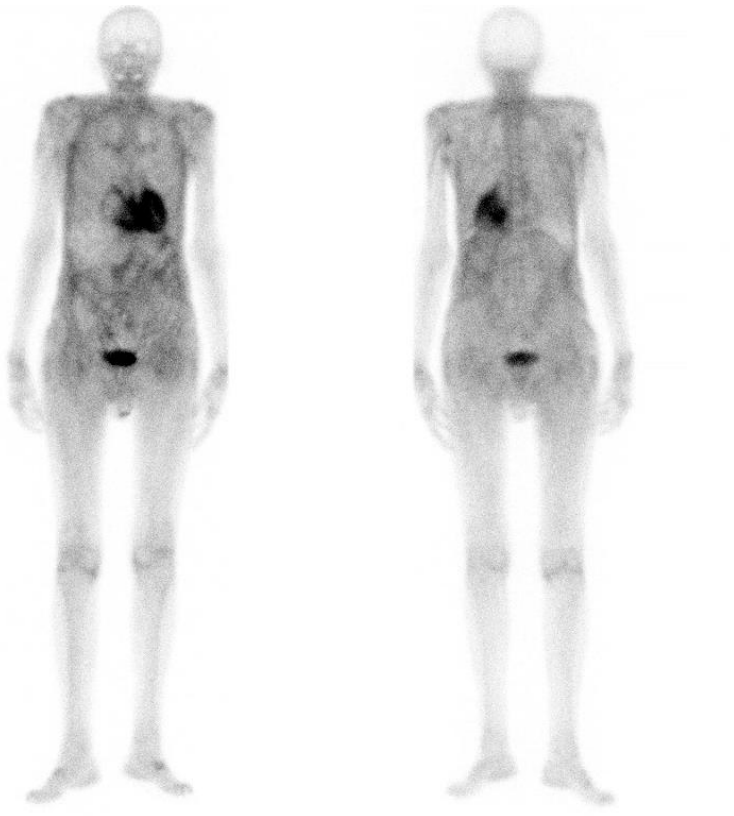

Fig. 6: A grade 3 patient with extensive ^{99m}Tc-DPD uptake in soft tissue. Uptake in underlying and overlying structures around the heart contribute unwanted counts.

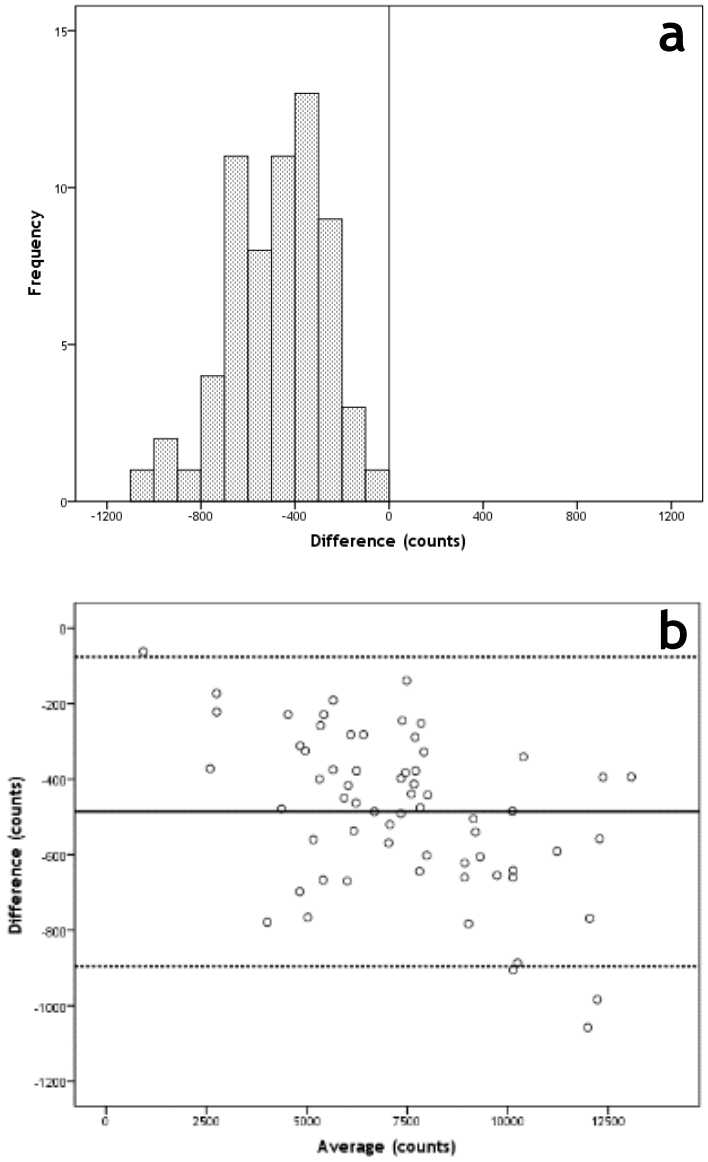

Fig. 7: (a) A histogram of differences; (b) a Bland-Altman plot, where the solid and dashed lines represent the mean, μ, and μ ± (1.96 × σ) respectively. A bias between the results of the OsiriX and Myovation™ methods was found, where smaller values were always generated with OsiriX

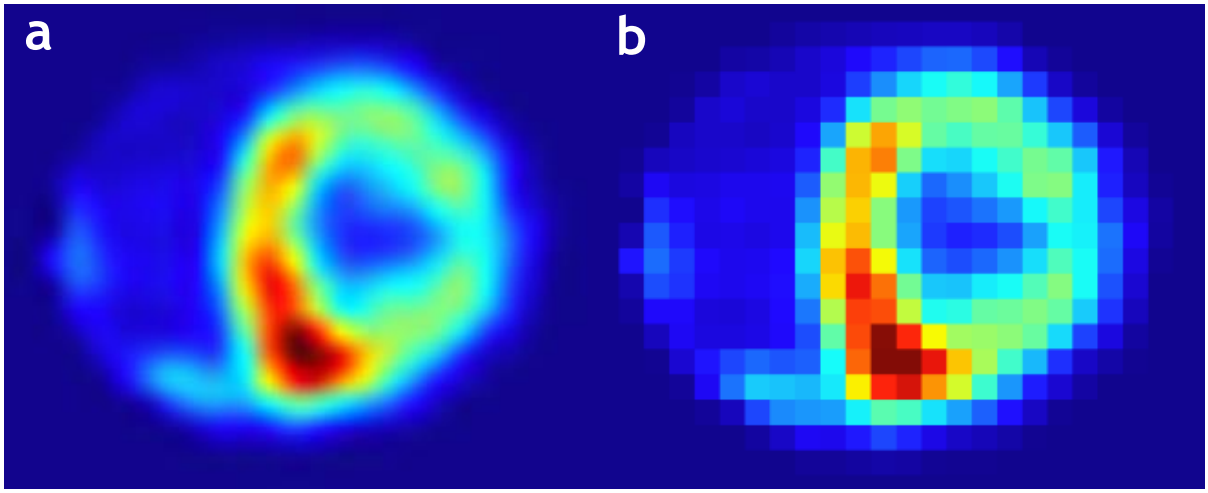

Fig. 8: ^{99m}Tc uptake visualised in OsiriX with (a) and without interpolation applied (b).

Word count

Abstract:

235

Main body (including titles, 37 references, captions, and tables but excluding ‘Notes’ and ‘Supplementary data’): 5058